Vascular Endothelial Growth Factor Receptor-1 Is Synthetic Lethal to Aberrant β-Catenin Activation in Colon Cancer

Snehal Naik, Robin S. Dothager, Jayne Marasa, Cory L. Lewis, and David Piwnica-Worms

Abstract

Purpose: The Wnt/β-catenin (β-cat) signaling cascade is a key regulator of development, and dysregulation of Wnt/β-cat contributes to selected cancers, such as colorectal, breast, and hepatocellular carcinoma, through abnormal activation of Wnt target genes. To identify novel modulators of the Wnt/β-cat pathway that may emerge as therapeutic targets, we did an unbiased high-throughput RNA interference screen.

Experimental Design: A synthetic oligonucleotide small interfering RNA library targeting 691 known and predicted human kinases was screened in Wnt3a-stimulated human cells in a live cell luciferase assay for modulation of Wnt/β-cat–dependent transcription. Follow-up studies of a selected high-confidence "hit" were conducted.

Results: A robust quartile-based statistical analysis and secondary screen yielded several kinases worthy of further investigation, including Cdc2L1, Lmtk3, Pank2, ErbB3, and, of note, vascular endothelial growth factor receptor (VEGFR)1/Flt1, a receptor tyrosine kinase (TK) with putative weak kinase activity conventionally believed to be a negative regulator of angiogenesis. A series of loss-of-function, genetic null, and VEGFR TK inhibitor assays further revealed that VEGFR1 is a positive regulator of Wnt signaling that functions in a glycogen synthase kinase-3β (GSK3β)–independent manner as a potential synthetic lethal target in Wnt/β-cat–addicted colon carcinoma cells.

Conclusions: This unanticipated non-endothelial link between VEGFR1 TK activity and Wnt/β-cat signaling may refine our understanding of aberrant Wnt signaling in colon carcinoma and points to new combinatorial therapeutics targeted to the tumor cell compartment, rather than angiogenesis, in the context of colon cancer. (Clin Cancer Res 2009;15(24):7529–37)

The Wnt signal transduction cascade relays progrowth signals through β-catenin (β-cat), a key transcriptional coactivator whose cellular levels are tightly regulated. In nonactive states, serine/threonine phosphorylation of β-cat by glycogen synthase kinase-3β (GSK3β), the component kinase of the adenomatous polyposis coli–mediated destruction complex, results in β-cat polyubiquitination mediated by the E3 ligase β-TrCP and consequent proteasomal degradation. In the presence of activating Wnt ligands, the destruction complex is inhibited, and an active β-cat population accumulates in the cytoplasm and translocates into the nucleus, where it forms a transactivator complex with lymphoid-enhancing factor or T-cell factor, resulting in the transcription of >50 target genes (1, 2). Aberrant activation of the Wnt pathway resulting in ligand-independent signaling and constitutively high levels of Wnt target gene expression is common in colon cancers (1, 2). Although such Wnt/β-cat activation contributes to certain forms of cancer, it may also create therapeutically exploitable vulnerabilities within the context of synthetic lethality (3, 4). Two genes are classically synthetic lethal if cells with a mutation in either one of the genes are viable, but simultaneous mutation of both genes causes death or impairs cellular fitness (5, 6). The idea can be extended to common mechanisms of cancer transformation, such as gain-of-function oncogenes exemplified by aberrant Wnt/β-cat activation. In this regard, inhibition or mutation of a second gene may be lethal or antiproliferative only in the context of specific oncogenic upregulation (3). Thus, it may be possible to use the contextual difference of aberrant Wnt/β-cat activation to find selective targets for therapeutic intervention. Kinases, an important family of functional regulators, have emerged as therapeutically alluring targets because single kinase inhibition can often eliminate an entire stimulatory or inhibitory arm of a signal transduction cascade. We have generated a screening strategy

Authors' Affiliation: Molecular Imaging Center, Mallinckrodt Institute of Radiology, and Department of Developmental Biology, Washington University School of Medicine, St. Louis, Missouri

Received 2/9/09; revised 8/31/09; accepted 9/16/09; published online 12/15/09.

Grant support: NIH grant P50 CA94056 (D. Piwnica-Worms), the Siteman Cancer Center at Washington University School of Medicine through National Cancer Institute Cancer Center Support Grant P30 CA091842 and an Anheuser-Busch/Emerson challenge gift, the Cancer Biology Pathway training program through the Siteman Cancer Center (S. Naik), and an American Cancer Society Postdoctoral Fellowship (R.S. Dothager).

The costs of publication of this article were defrayed in part by the payment of page charges. This article must therefore be hereby marked *advertisement* in accordance with 18 U.S.C. Section 1734 solely to indicate this fact.

Note: Supplementary data for this article are available at Clinical Cancer Research Online (http://clincancerres.aacrjournals.org/).

Requests for reprints: David Piwnica-Worms, Mallinckrodt Institute of Radiology, Washington University School of Medicine, St. Louis, MO 63110. Phone: 314-362-9359; Fax: 314-362-0152; E-mail: piwnica-wormsd@mir.wustl.edu.

doi:10.1158/1078-0432.CCR-09-0336

Translational Relevance

Activation of Wnt signaling, which is observed constitutively in most colon cancers, targets >50 genes by a transactivator complex comprising β-catenin (β-cat) and T-cell factor. To uncover novel kinases that modulate Wnt signal transduction and are essential to the survival of cells addicted to Wnt/β-cat signaling, we systematically inactivated, one at a time, all human genes that direct the synthesis of kinases in cells stimulated with Wnt. Our screen identified an unanticipated mode of cross-talk between vascular endothelial growth factor receptor (VEGFR)1/Flt1 and the Wnt/β-cat pathway, two pathways of tremendous importance in cancer. Initial mechanistic studies provided evidence for VEGFR1/Flt1-linked tyrosine phosphorylation of β-cat, thereby modifying transcriptional activity. Thus, a mechanistically rational strategy for synthetic lethal therapy in the treatment of colon carcinoma is targeted suppression of VEGFR1-linked tyrosine kinase activity within the Wnt/β-cat–addicted tumor cell compartment per se, not endothelia.

that combines the study of Wnt pathway activation with loss of individual kinases to uncover candidate kinase modulators that may emerge as therapeutic targets in the context of Wnt-addicted colon cancer.

Materials and Methods

Cell lines and reagents. *pCMV-FLuc* has been previously described (7). *pTOPFLASH* and *pcDNA3.1* were purchased from Upstate Products (Billerica, MA) and Invitrogen Corporation (Carlsbad, CA), respectively. STF293 reporter cells were kindly provided by Dr. Jeremy Nathans (Johns Hopkins University School of Medicine, Baltimore, MD) and cultured in STF293 medium. HEK293, HEK293T, and HeLa cells (ATCC, Manassas, VA) were cultured in DMEM supplemented with 10% heat-inactivated fetal bovine serum and 1% glutamine. SW480 and KM12L4a colon carcinoma cells (kindly provided by Dr. Loren Michel, Washington University School of Medicine, St. Louis, MO) were cultured in DMEM supplemented with 10% fetal bovine serum and 1% glutamine. L cells and L Wnt-3a cells were purchased from ATCC, and conditioned medium was collected according to the ATCC protocol. A HEK293 cell line stably expressing FLuc (293Luc) was established by transfecting 293 cells with *pCMV-FLuc* with the use of FuGENE 6 transfection reagent (Roche, Indianapolis, IN) for 48 h followed by selection of single colonies after continuous exposure to G418 (0.4 mg/mL). SB216763 (Sigma-Aldrich, St. Louis, MO), and VEGFR tyrosine kinase (TK) inhibitors II and III (EMD Biosciences, Gibbstown, NJ) were reconstituted in DMSO. Plasmids expressing short hairpin RNA (shRNA) sequences were provided by the Genome Sequencing Center, Washington University School of Medicine. Each sequence was provided in a *pLKO.1* expression vector.

High-throughput screening. Small interfering RNA (siRNA) screening was done in black, clear-bottomed, 96-well culture plates (Corning 3904) with the use of a Beckman Coulter (Fullerton, CA) Core Robotics system, including an FX liquid handler, controlled by the Sagian graphical method development tool (SAMI scheduling software). STF293 cells (10,000 per well) in STF293 medium (DMEM/F12 supplemented with 10% heat-inactivated fetal bovine serum and 1% glutamine) at 100 μL/well were seeded 1 d before transfection. Plates were maintained in an environmentally controlled Cytomat incubator until use, thereby optimizing health and ensuring uniform treatment of all plates. Forward transfection was done with a 96-channel head on the FX liquid handler, adding 0.2 μL/well of media-complexed DharmaFECT 1 reagent (Dharmacon Research Inc., Valencia, CA) to the aliquoted siRNA library (Kinase siRNA set v2; Qiagen Inc., Valencia, CA) in a 96-well reaction plate. Experimental siRNA oligos were arrayed in columns 2 to 11 of each plate, and individual controls comprising mock-transfected wells, a nontargeting siControl sequence (Dharmacon Research Inc., Lafayette, CO), as well as a firefly luciferase–targeting siRNA sequence (Dharmacon Research Inc.) were placed manually in columns 1 and 12. After incubation of siRNA-DharmaFECT 1 complexes for 20 min at room temperature, 100 μL of the complexed siRNA was added to each well of a plate with cells (×3 plates) with the use of the FX liquid handler, yielding a final concentration of ~25 nmol/L siRNA per well. Plates were maintained in the Cytomat for 24 h, after which each plate was aspirated with the use of the BioTek (Winooski, VT) ELx405 Select microplate washer. Wnt3a-conditioned media (200 μL/well) containing 150 μg/mL D-luciferin (Biosynth, Naperville, IL) was added with the use of the FX liquid handler, and cells were incubated for 10 min. The luminescent signal was measured under ultrasensitive detection mode on an EnVision plate reader (PerkinElmer, Waltham, MA) 10 min, and 6, 12, and 18 h post Wnt3a addition. Cell viability was then determined with resazurin dye (Sigma R7017; final concentration, 44 μmol/L) after 90-min incubation at 37°C, as monitored on a FLUOstar OPTIMA fluorescence reader (BMG Labtech, Cary, NC; excitation, 544 nm; emission, 590 nm).

Secondary shRNA screen. STF293 cells in DMEM/F12 media supplemented with 10% heat-inactivated fetal bovine serum and 1% glutamine were plated in 24-well or 96-well plates 1 d before transfection such that cells would be ~70% confluent on the day of transfection. In quadruplicate, cells were transfected with 800 ng (for 24-well plates) or 300 ng (for 96-well plates) of shRNA expression vector. Four individual shRNA sequences (except three for Pank2) that targeted nonoverlapping segments of the coding region of each original high stringency "hit" gene were used. Also included were a nontargeting scrambled sequence (negative control) and a sequence targeting firefly luciferase (positive control). Plasmids were transfected with the use of Lipofectamine 2000 at a 2.5:1 ratio (volume of reagent to micrograms of DNA) in 100 μL (for 24-well plates) or 50 μL (for 96-well plates) of serum-free DMEM/F12 media. Transfection reagent was added to the serum-free media and incubated for 5 min, followed by addition of DNA. After incubation for 20 min, the transfection mixture was added dropwise to wells of assay plates. Cells were incubated in the transfection mixture for 4 h, and then the media was replaced with fresh DMEM/F12 media containing serum. After transfection, cells were incubated for 24 h followed by doubling of the volume in each well by addition of Wnt3a-conditioned media that contained 150 μg/mL of D-luciferin. Cells were incubated for another 24 h and then imaged on a bioluminescence imaging system (IVIS 100, Caliper Life Sciences, Hopkinton, MA; filter, open; f-stop, 1; exposure, 5 min; binning, 8). After bioluminescence imaging, an MTS cell viability assay was done (CellTiter 96 AQueous One Solution Cell Proliferation Assay, Promega, Madison, WI) by measuring the formation of the formazan product (absorbance at 490 nm, 1 h, 37°C) with the use of a FluoStar Optima plate reader for 24-well plates or an EL 311 plate reader (BioTek Instruments) for 96-well plates.

RT^2 Profiler PCR Wnt Array. Embryonic stem cells from wild-type R1 or *VEGFR1/Flt1*$^{(-/-)}$ mice were provided by Dr. Guo-Hua Fong (University of Connecticut Health Center, Farmington, CT) and Dr. Kyunghee Choi (Washington University School of Medicine), and maintained at the Murine Embryonic Stem Cell Core at Washington University. Cells were cultured in DMEM containing FCS, L-glutamine, nonessential amino acids, HEPES, leukemia inhibitory factor, and 2-mercaptoethanol, and plated on gelatinized 10-cm tissue culture dishes to eliminate mouse embryonic fibroblasts before experimental assays. After incubation of embryonic stem cells in the presence or absence of rWnt3a, RNA was obtained with the use of the RNeasy RNA extraction kit (Qiagen), including the optional DNase digestion protocol. Reverse transcriptase-PCR array profiling was done with the use of the pathway-specific RT^2 Profiler PCR Array system (SuperArray, Frederick, MD)

according to the manufacturer's instruction, in an ABI 7300 real-time PCR system (Applied Biosystems, Foster City, CA). Data analysis with the use of the ΔC_t method was done according to a data analysis template available online.[1] Briefly, ΔC_t values were calculated by subtracting the average cycle threshold (C_t) values for housekeeping genes (glyceraldehyde-3-phosphate dehydrogenase, β-actin, and Hprt1) from the C_t values for T (Brachyury). Fold differences were calculated as $2^{-\Delta C}t$ (rWnt3a treated)/$2^{-\Delta C}t$ (untreated) for both wild-type and *VEGFR1*$^{(-/-)}$ embryonic stem cells.

Semiquantitative reverse transcriptase-PCR. siRNA transfections were done as described above and allowed to proceed for 48 h. RNA was extracted with the use of a RNeasy RNA extraction kit (Qiagen). One-step reverse transcriptase-PCR was done according to the manufacturer's protocol with the use of the Access RT-PCR system (Promega) on a GeneAmp PCR system 2700 (Applied Biosystems). The primer sequences were as follows: VEGFR1 extracellular domain, forward primer TGGGACAGTAGAAAGGGCTT, reverse primer GGTCCACTCCTTACACGACAA; glyceraldehyde-3-phosphate dehydrogenase, forward primer GTGAAGGTCGGAGTCAACGG, reverse primer TGATGACAAGCTTCCCGTTCTC. Amplified products were subjected to agarose gel electrophoresis, and visualized as a 384-bp product for VEGFR1 and a 200-bp product for glyceraldehyde-3-phosphate dehydrogenase with the use of a ChemiImager (Alpha Innotech Corp., San Leandro, CA).

In cellulo *transfection assays.* In STF293 cells, follow-up siRNA validation studies were done with the use of a forward transfection protocol with DharmaFECT 1 reagent (Dharmacon Research Inc.) at a final concentration of 50 nmol/L siRNA (ON-TARGETplus SMARTpool, L-003136-00; Dharmacon Research Inc.), and 20 nmol/L siRNA (individual duplexes; Dharmacon Research Inc.). In other experiments, cells were transfected with *pTOPFLASH* with the use of Lipofectamine 2000 (Invitrogen) according to the manufacturer's instructions. Bioluminescence was captured with the use of an IVIS 100 or IVIS 50 imaging system, and Living Image (Caliper Life Sciences) and Igor (WaveMetrics, Lake Oswego, OR) software. The acquisition variables were as follows: no filter; exposure time, 1 to 2 min; binning, 8; f-stop, 1; field of view, 12 (IVIS 50) or 10 cm (IVIS 100).

MTS assays. STF293, HeLa, KM12l4a, and SW480 (1,000 cells per well) were plated in appropriate media in clear 96-well plates. Numerous wells containing medium only were also plated as background controls. Each cell line was treated with increasing drug concentrations in triplicate, whereas STF293 cells were also treated with Wnt3a together with increasing drug concentrations. Drug treatment proceeded for 72 h, after which MTS reagent (Promega) was added and incubated for 1 to 3 h depending on the cell line, and the absorbance was assayed at 490 nm in an EL 311 plate reader (BioTek Instruments). Background subtraction was done from medium-only wells that had each been treated with the corresponding drug concentrations in duplicate to calculate the corrected absorbance. Data were then normalized as fold drug-untreated values for each cell type to facilitate plotting on the same graph.

Immunofluorescence and confocal microscopy. Cells were transfected (for siRNA assays) or treated (for Inh II assays) in 35-mm glass coverslip dishes (MatTek Cultureware), and treated with Wnt3a or control media for 2 h before fixation in 4% paraformaldehyde solution. Samples were then washed, treated with ice-cold methanol for 10 min at -20°C, washed, and incubated with anti–β-cat antibody (BD Biosciences; 1:500 dilution) overnight at 4°C on a rocking platform. After three washes, a 2-h incubation in Alexa 488–conjugated secondary antibody (Invitrogen Corporation; 1:500 dilution) was done at room temperature in the dark. Samples were incubated with 10 μg/mL of 4′, 6-diamidino-2-phenylindole for 15 min in the dark and stored in PBS at 4°C protected from light. Images (10 μm slice thickness; ×40 magnification) were acquired with the use of an inverted Zeiss Axiovert 200 laser scanning confocal microscope coupled to a Zeiss LSM 5 PASCAL fitted with excitation lasers at 488 nm (for β-cat) and 405 nm (for 4′, 6-diamidino-2-phenylindole), and long pass emission filters at 505 nm (for β-cat) and 420 nm (for 4′, 6-diamidino-2-phenylindole).

Immunoprecipitation and Western blotting. Cells were transfected (for siRNA assays) or treated (for Inh II assays) in 10-cm tissue culture–treated dishes, and harvested in immunoprecipitation buffer [50 mmol/L HEPES (pH 7.5), 150 mmol/L NaCl, 5% glycerol, 1% Triton X-100, 1 mmol/L EDTA, 10 mmol/L NaF, and 30 mmol/L glycerol phosphate] freshly combined with a 1:100 dilution of protease inhibitor cocktail (Sigma-Aldrich) and a 200-μmol/L final concentration of sodium orthovanadate. Protein amounts were quantified with the use of a bicinchoninic acid assay (Pierce, Rockford, IL) according to the manufacturer's protocol. Protein (500 μg) from each sample was incubated for 1 h with anti–β-cat antibody (BD Biosciences; 0.5 μg) on a rocking platform and then complexed with Protein A agarose beads (Calbiochem, La Jolla, CA) overnight at 4°C on a rotator. Samples were washed thrice after centrifugation at 6,000 rpm and boiled for 10 min before separation by SDS-PAGE. After transfer to a polyvinylidene difluoride membrane, blocking was allowed to proceed for 2 h at room temperature, followed by incubation with anti-phosphotyrosine antibody (clone 4G10; Upstate Products; 1:1,000 dilution) overnight at 4°C. Immune complexes were detected by horseradish peroxidase–labeled secondary antibodies and enhanced chemiluminescence reagent (Amersham Biosciences). Exposure and densitometric analysis were done with the use of the IVIS imaging system, and Living Image (Caliper Life Sciences) and Igor (WaveMetrics) software. A similar SDS-PAGE and immunoblotting protocol was followed for detection of β-cat (1:200 dilution), VEGFR1 (1:200 dilution), and actin (1:1,000 dilution) with the use of antibodies from Santa Cruz (Santa Cruz, CA), Chemicon Corporation (Billerica, MA), and Sigma-Aldrich, respectively.

Statistical analysis and hit selection. In the primary siRNA screen, the luminescence data acquired 18 h post Wnt3a treatment were normalized to cell viability data (expressed as value = ×). Median (Q2), first (Q1), and third (Q3) quartile values were calculated for all normalized values and subjected to plate-by-plate analysis. To facilitate experiment-wide analysis, further normalization was done with a control nontargeting siRNA placed on each individual assay plate. Q1, Q2, and Q3 values were calculated as described above. Averages and SE calculations were done for triplicates of log(x/median) values. Upper and lower boundaries were calculated as Q3 + 2c(Q3 - Q2) and Q1 - 2c(Q2 - Q1), respectively, for c = 1.7239, corresponding to a high stringency targeted error rate ($\alpha = 0.0027$), and c = 0.9826, corresponding to a lower stringency targeted error rate ($\alpha = 0.046$; ref. 8). High stringency hits were chosen as those targets that scored $\alpha \leq 0.0027$ in both plate-by-plate and experiment-wide analyses. Selected targets clustered within the first two plates (numbers 1-150; Fig. 1, *red circles*) represented hits scored as significant based on the high stringency criteria in an experiment-wide analysis only and not in a plate-by-plate analysis (listed in Supplementary Table S3). This ensued from the alphabetical clustering and nonrandom placement of siRNA sequences on the plates by the vendor, resulting in over-representation of hits in the first two plates, thereby infringing on the sparse-hit hypothesis, which assumes that hits are randomly spaced throughout the dataset.

Experimental statistical analyses. Student's *t* tests, two-way ANOVA, curve fitting, box plots, and IC_{50} calculations were done with the use of GraphPad software (GraphPad, La Jolla, CA).

Results

Kinase-targeted high-throughput siRNA screen of Wnt/β-cat–dependent transcription. We used a synthetic oligonucleotide siRNA library targeting known and predicted human kinases in a high-throughput screening format for systematic yet unbiased target discovery in contexts that were both physiologically relevant and therapeutically alluring (3, 4). HEK293 cells stably expressing a luciferase transcriptional reporter of Wnt/β-cat target gene activation (STF293 cells; ref. 9) were transfected with

[1] http://www.sabiosciences.com/pcrarraydataanalysis.php

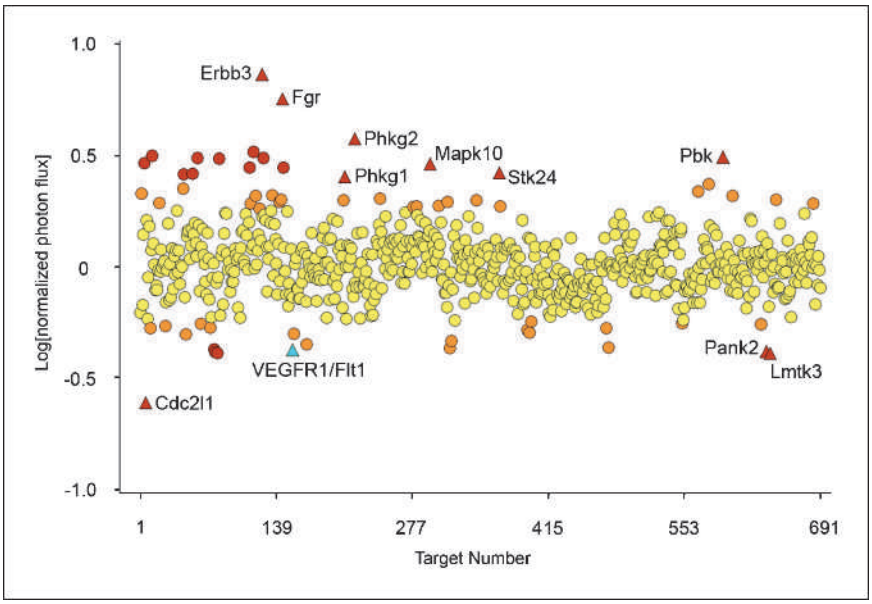

Fig. 1. High-throughput RNA interference screen for kinase modulators of Wnt signaling. Screen results including hits at various significance thresholds. Log(normalized photon flux) represents bioluminescence reporter signal intensity normalized for cell viability and a control nontargeting sequence placed on each plate to facilitate experiment-wide analysis. Values are plotted for siRNA against all 691 kinase targets. Log(normalized photon flux) values of <-0.37 and >0.38 score as significant based on high stringency criteria ($\alpha \leq 0.0027$; *red*). Values between -0.37 and -0.25, and between 0.38 and 0.26, score as significant based on lower stringency criteria ($\alpha \leq 0.046$; *orange*). *Red triangles*, hits scored at $\alpha \leq 0.0027$ in both experiment-wide and plate-by-plate analyses (Supplementary Table S1); blue triangle, VEGFR1/Flt1. *Red circles*, hits that score as significant based on high stringency criteria in experiment-wide analysis only and not in plate-by-plate analysis (listed in Supplementary Table S3). For details on the quartile-based statistical analysis see Materials and Methods; siRNA sequences targeting genes identified as high stringency hits (*triangles*) in the primary screen are listed in Supplementary Table S4.

1,382 siRNA duplexes targeting 691 distinct genes as a pool of 2 duplexes per target in a 96-well high-throughput screen (Supplementary Fig. S1), and subsequently treated with Wnt3a-conditioned media (Wnt3a; ref. 10) to emulate pathway activation. Human cells, together with a functionally targeted synthetic oligonucleotide library, were used to maximize the discovery of potential disease-relevant candidates and minimize off-target effects, such as those that can be observed in genome-wide screens conducted in model organisms (11, 12). A highly stringent targeted error rate in a quartile-based analysis (ref. 8; see Materials and Methods) was used to uncover candidates of statistical relevance (Fig. 1). Eleven kinases (Cdc2L1, Pank2, Lmtk3, Flt1, ErbB3, Fgr, Mapk10, Phkg1, Phkg2, Pbk, and Stk24), representing both serine/threonine and TKs, were recovered as hits, all of which were kinases not previously associated with the Wnt pathway (Supplementary Table S1). Importantly, analysis at lower stringency revealed additional kinases, several of which have known Wnt pathway regulatory functions (transforming growth factor-β receptor, NLK, CK1/2, CDKN2a, AKT2/3, and GSK3α/β), which served to authenticate the screen (Supplementary Fig. S2; Supplementary Table S2). Also, a subset of kinases enriched in cell cycle regulators emerged from an experiment-wide analysis, including the noteworthy genes Cdk8 (13), ATM, and Plk3 (Supplementary Table S3). The loss of one subset of kinases (Cdc2L1, VEGFR1/Flt1, Pank2, and Lmtk3) resulted in reduced β-cat–dependent transcription (Fig. 1), representing potential targetable therapeutic genes.

Validation of hit genes with the use of shRNA knockdown. To validate the changes in Wnt/β-cat signaling that were observed in the primary screen, we rescreened in STF293 cells the 11 hit genes with the use of four separate shRNA sequences corresponding to each gene of interest. Plasmids bearing shRNA were chosen for the secondary screen because of their potential for higher potency, fewer off-target effects, and stability. The shRNA sequences were selected for those that target nonoverlapping segments of the coding regions of hit genes and were assessed individually as opposed to being pooled, as was done in the primary siRNA screen. Genes were qualified as reproducible if, in at least two of three separate experiments, ≥2 shRNA sequences for a target gene increased or decreased luciferase signals above or below the median of a nontargeting negative control shRNA in concordance with the trend previously observed with siRNA (see Fig. 2, which illustrates a representative experiment). Overall, shRNA against 5 of the original 11 hit genes showed the same effect on luciferase signal as was observed in the

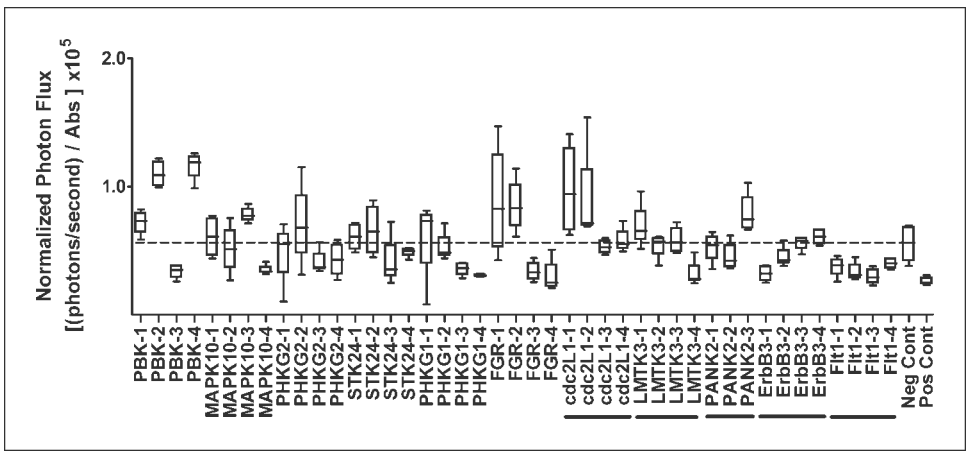

Fig. 2. Validation of Wnt/β-cat signaling changes after shRNA knockdown of hits. Box and whisker plot of one representative experiment showing luciferase reporter signal changes in STF293 cells 48 h after transfection with shRNA plasmids. Four different shRNA sequences targeting nonoverlapping segments of the coding regions of the indicated genes were tested in quadruplicate (*x*-axis). The photon flux in each well was normalized for cell viability (absorbance; Abs). *Lines*, medians; *boxes*, 25th to 75th percentile interquartile ranges; *whiskers*, the highest and lowest values for each replicate within a given gene. *Dashed horizontal line*, the median value of a negative control; *underline*, genes reproducible across at least two of three independent experiments.

primary screen, and were deemed reproducible: Cdc2L1, Lmtk3, Pank2, ErbB3, and VEGFR1/Flt1. Only VEGFR1/Flt1 was concordant in all three independent experiments.

Characterization of VEGFR1/Flt1 as a "high-confidence hit". Direct therapeutic applications may be found for candidates whose loss-of-function by RNA interference results in attenuated Wnt/β-cat signaling, especially in the context of "oncogene-addicted" colon cancer cells, in which the loss of aberrantly active Wnt/β-cat signaling results in decreased cell survival (14). In this regard, the specific identification of VEGFR1/Flt1, but not VEGFR2/KDR or VEGFR3/Flt4, as a "reproducible hit" was striking. VEGFR1, a receptor TK with putative weak kinase activity, is conventionally thought to function as a negative regulator of angiogenesis (15, 16), an endothelial cell process that is actively targeted in the treatment of colorectal cancers (17). To extend the cellular link between VEGFR1 function and Wnt/β-cat signal transduction, we further validated the effects of VEGFR1 knockdown on the β-cat–dependent transcription observed in the primary screen. With the use of STF293 cells, a pool of four independently designed sequences against VEGFR1, as well as three of these four when tested as individual siRNA sequences, resulted in knockdown of VEGFR1 (Fig. 3A) and again attenuated β-cat–dependent transcriptional activation (Fig. 3B and C), confirming the primary screen. No effect was observed in control HEK293-Luc cells (293Luc), a line expressing luciferase from a constitutive non–β-cat–responsive cytomegalovirus promoter (Fig. 3D).

To independently confirm that the absence of VEGFR1 resulted in attenuated Wnt signaling at the level of transcriptional activation of Wnt/β-cat targets, we obtained embryonic stem cells derived from a *VEGFR1*$^{(-/-)}$ mouse (18). Importantly, quantitative reverse transcriptase-PCR–based profiling for genes implicated in Wnt signaling was done in both wild-type and *VEGFR1*$^{(-/-)}$ embryonic stem cells. Embryonic stem cells lacking *VEGFR1* and treated with rWnt3a showed a mere 5-fold increase in expression of T (Brachyury), a specific transcriptional target of Wnt3a in embryonic stem cells [ref. 19; $2^{-\Delta C}$t values: 4.5e-02 (treated) versus 8.6e-03 (untreated)]. By comparison, in rWnt3a-treated wild-type embryonic stem cells, a robust 44-fold increase in T was observed [$2^{-\Delta C}$t values: 6.2e-02 (treated) versus 1.4e-03 (untreated)]. These data provided strong evidence that VEGFR1 enhanced Wnt signaling in embryonic stem cells.

Inhibition of VEGFR1 TK activity inhibits Wnt/β-cat–dependent transcription and is synthetic lethal in colon cancer cells. Recent data indicate that the expression of VEGFR1 in primary colon carcinoma tumor samples correlates with disease progression (20). However, the mechanistic basis of this observation has not been elucidated. Thus, to directly test the effect of abrogating VEGFR TK activity on cell survival, SW480 and KM12L4a cells, colon cancer lines that show constitutive β-cat activation (21), were treated with VEGFR TK inhibitor II (ref. 22; Inh II) for 72 hours (Fig. 4A). An Inh II–induced decrease in the MTS cell viability assay was seen in these Wnt/β-cat–addicted colon cancer cells in a concentration-dependent manner. The observed IC_{50} of 336 nmol/L (for SW480) and 120 nmol/L (for KM12L4a) matched the known IC_{50} for inhibition of VEGFR1 TK activity (180 nmol/L), a value 9-fold greater than the IC_{50} for inhibition of VEGFR2 TK activity (20 nmol/L; ref. 22). In contrast, a 72-hour MTS assay with STF293 cells, a line that exhibits normal Wnt signaling, was unaffected by Inh II even in the presence of Wnt stimulation. Furthermore, cervical carcino-

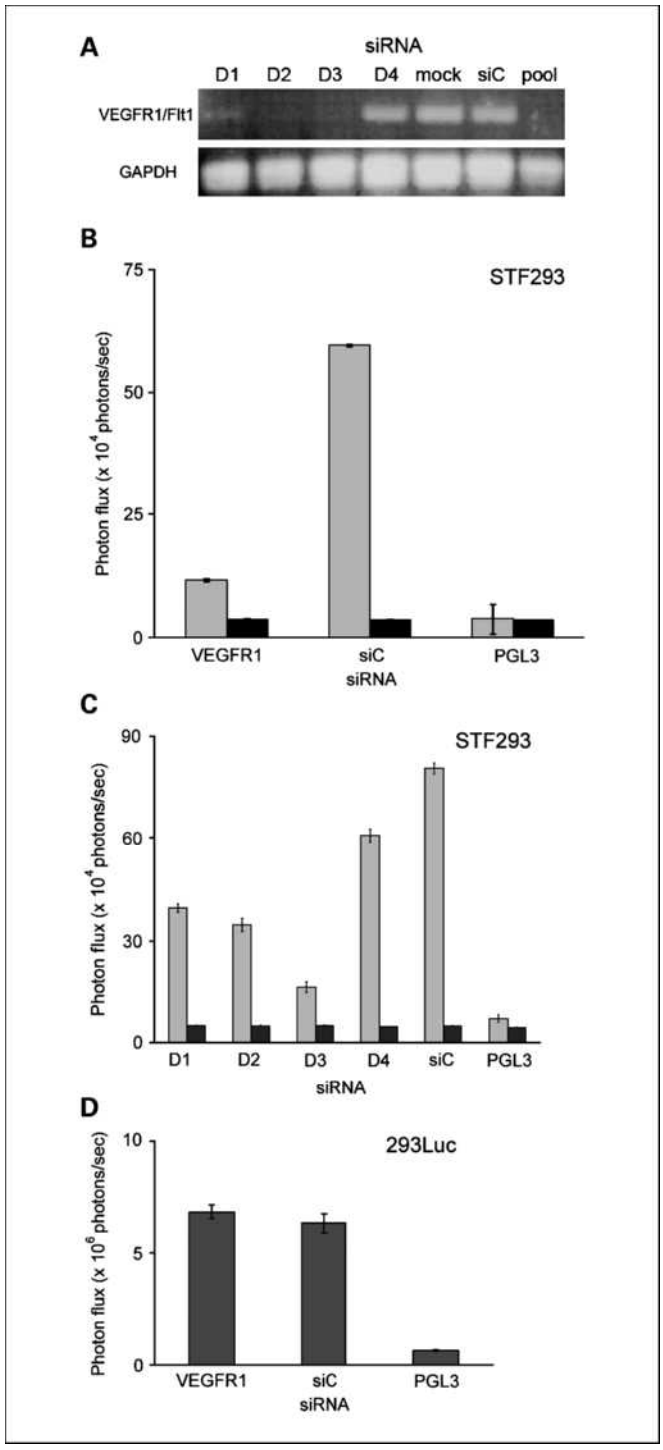

Fig. 3. Validation of negative regulation of Wnt/β-cat signaling upon loss of VEGFR1 with the use of pooled and individual siRNA duplexes targeting VEGFR1. *A*, gel electrophoresis after semiquantitative reverse transcriptase-PCR from STF293 cells mock-transfected (mock) or transfected with individual duplexes (D1-D4) targeting VEGFR1, a nontargeting siControl sequence (siC), or a set of four pooled ON-TARGETplus sequences against VEGFR1 (pool). Gene-specific primers were used to amplify VEGFR1 or control glyceraldehyde-3-phosphate dehydrogenase (GAPDH). Effect of (*B*) a set of four pooled siRNA sequences against VEGFR1 or (*C*) individual sequences (D1-D4) targeting VEGFR1, along with nontargeting siC as well as a firefly luciferase (PGL3)-targeting siRNA on STF293 cells stimulated with Wnt3a (*gray*) or control media (*black*). Data, mean photon flux ± SE ($n = 3$ per condition). *D*, knockdown of VEGFR1 had no effect on control 293Luc cells expressing a non–Wnt-dependent reporter, both in the absence (shown) or presence of Wnt3a.

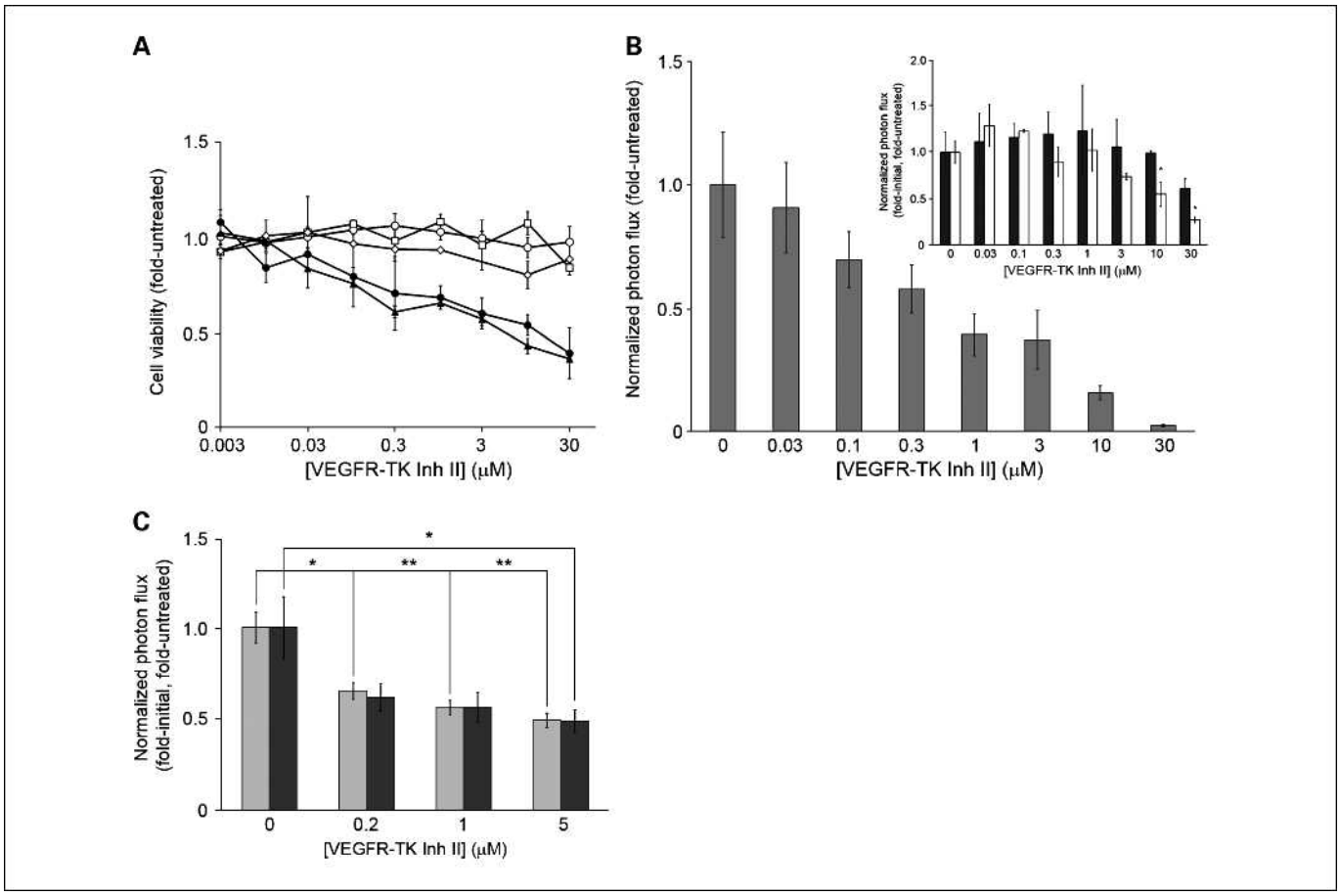

Fig. 4. Inhibition of VEGFR TK activity is synthetic lethal in β-cat–addicted colon cancer cells, acting through downregulation of Wnt/β-cat–dependent transcriptional activation. *A,* inhibition of VEGFR TK activity selectively diminishes the viability of SW480 (*filled circle*) and KM12L4a (*filled triangle*) colon cancer cells, but not Wnt3a-stimulated STF293 cells (*open square*), control STF293 cells (*open diamond*), or non–colon cancer HeLa cells (*open circle*). Each cell type was treated with increasing concentrations of Inh II for 72 h before cell viability analysis with the use of an MTS assay. Data, mean ± SE of fold untreated absorbance values from two independent experiments ($n = 3$ each) for each concentration for each cell line. *B,* reporter concentration response in STF293 cells stimulated with Wnt3a after pretreatment with increasing concentrations of Inh II. The bioluminescence photon flux was normalized to cell viability with the use of a resazurin dye–based fluorescence assay and plotted as fold untreated normalized photon flux ± propagated SE ($n = 3$ per concentration). *Inset*, in HEK293T cells transfected with *pTOPFLASH*, Inh II strongly attenuated β-cat–dependent transcription induced by Wnt3a (*white bars*) but showed a statistically significant lower effect on basal transcriptional activity in the absence of Wnt3a (*black bars*). The bioluminescence photon flux was normalized to cell viability with the use of a resazurin dye–based fluorescence assay and plotted as fold initial, fold untreated normalized photon flux ± propagated SE ($n = 3$ per concentration). *, $P < 0.05$, Student's *t* test. Two-way ANOVA also found statistically significant effects of both Wnt treatment ($P < 0.05$) and drug concentration ($P < 0.001$). *C,* inhibitory effect of 48-h exposure to increasing concentrations of Inh II on constitutively active β-cat–dependent signaling in SW480 (*gray bars*) and KM12L4a (*black bars*) colon carcinoma cells transfected with *pTOPFLASH*. Data, mean fold-initial, fold-untreated photon flux ± propagated SE ($n = 3$ per concentration). *, $P < 0.05$; **, $P < 0.01$, Student's *t*-test.

ma–derived HeLa cells, a line that does not exhibit aberrant Wnt/β-cat pathway activation (23), also showed no response to Inh II (Fig. 4A). These data suggested that VEGFR TK inhibition was synthetic lethal to cells with aberrant Wnt/β-cat signaling, a process essential for colon cancer cell survival (24), but not to cells with normal Wnt/β-cat signaling. However, further analysis of the luciferase transcriptional reporter showed that treatment with Inh II still resulted in a concentration-dependent inhibition of canonical β-cat–dependent transcription in STF293 cells (Fig. 4B) but only in the presence of Wnt3a, as confirmed by transient transfection of HEK293T cells with *pTOPFLASH*, a similar β-cat–dependent bioluminescence reporter to that used in STF293 cells (Fig. 4B, *inset*). Finally, in SW480 and KM12L4a colon cancer cells transiently transfected with the *pTOPFLASH* reporter, constitutively active β-cat–dependent transcription was also attenuated upon treatment with Inh II (Fig. 4C). These effects were recapitulated with VEGFR TK inhibitor III, a second inhibitor targeting VEGFR TK activity (ref. 25; Supplementary Fig. S3A and B), but no effects were observed in off-target transcriptional reporter cells (293Luc) as expected (data not shown). Thus, whereas inhibition of VEGFR1 TK activity blocked Wnt-induced β-cat–dependent transcription in normal cells as well as constitutively active β-cat–dependent transcription in colon cancer cells, it was only in colon cancer cells that VEGFR1 TK blockade was lethal. Overall, with the caveat that the pharmacologic specificity of the tested inhibitors is not fully resolved, these data showed that by targeting VEGFR1 TK activity, the therapeutically exploitable vulnerability of Wnt/β-cat–addicted colon carcinoma was exposed.

Wnt pathway modulation by VEGFR1 is independent of GSK3β-dependent β-cat stabilization. Mutations in APC or β-cat are prevalent in colon carcinoma, resulting in constitutively stabilized β-cat that is no longer a substrate for GSK3β (1, 2). Concordantly, in STF293 cells in which β-cat was stabilized by pharmacologic treatment with the GSK3β inhibitor SB216763 (10 μmol/L; ref. 26), knockdown of VEGFR1 with duplexes of

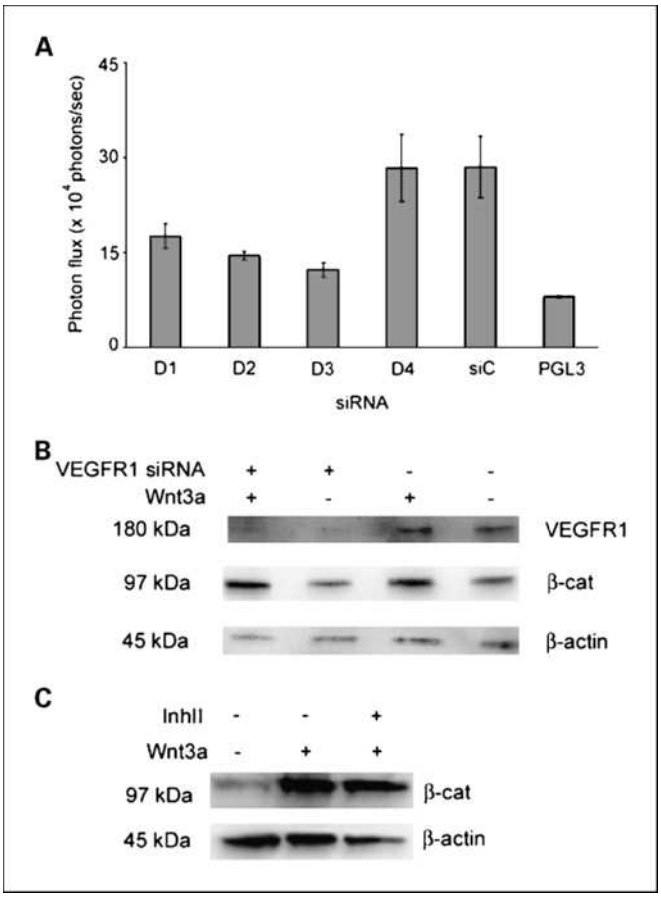

Fig. 5. VEGFR1 acts in a GSK3β-independent manner and downstream of β-cat protein stabilization. *A,* effects of individual duplexes (D1-D4) targeting VEGFR1, a nontargeting siControl sequence (siC) and a firefly luciferase–targeting (PGL3) siRNA on STF293 cells treated with the GSK3β inhibitor SB216763 (10 μmol/L). Bioluminescence photon flux, mean photon flux ± SE ($n = 4$). *B,* western blot analysis of STF293 cells transfected with ON-TARGETplus SMARTpool siRNA targeting VEGFR1 (*lanes 1* and *2*) or off-target PGL3-targeting siRNA (*lanes 3* and *4*), and stimulated with Wnt3a (*lanes 1* and *3*) or control media (*lanes 2* and *4*), or (*C*) treated with vehicle (*lanes 1* and *2*) or 1 μmol/L VEGFR TK Inh II (*lane 3*) for 18 h together with control media (*lane 1*) or Wnt3a (*lanes 2* and *3*).

siRNA yielded a similar attenuation of β-cat–dependent transcription (Fig. 5A) as VEGFR1 knockdown in the context of Wnt3a stimulation (Fig. 3C). Thus, the effect of VEGFR1 was independent of GSK3β.

Downstream processing. VEGFR1 did not seem to impact the processing of total β-cat protein levels. For example, Western blot analysis of STF293 cells showed competent stabilization of β-cat protein upon stimulation with Wnt3a, even when effective knockdown of VEGFR1 protein was achieved with siRNA (Fig. 5B) or VEGFR TK activity was blocked (Fig. 5C). Overall, these data would suggest that therapeutic interventions directed at VEGFR TK activity may be mechanistically impacting downstream processing nodes of the Wnt/β-cat pathway within cells, such as nuclear translocation or transcriptional activation.

We thus explored the effect of VEGFR1 on nuclear translocation of β-cat with the use of immunofluorescence microscopy. In STF293 cells, both VEGFR1 knockdown with siRNA (Fig. 6A) or pharmacologic inhibition of VEGFR TK activity with Inh II (Fig. 6B) resulted in normal Wnt-induced β-cat accumulation

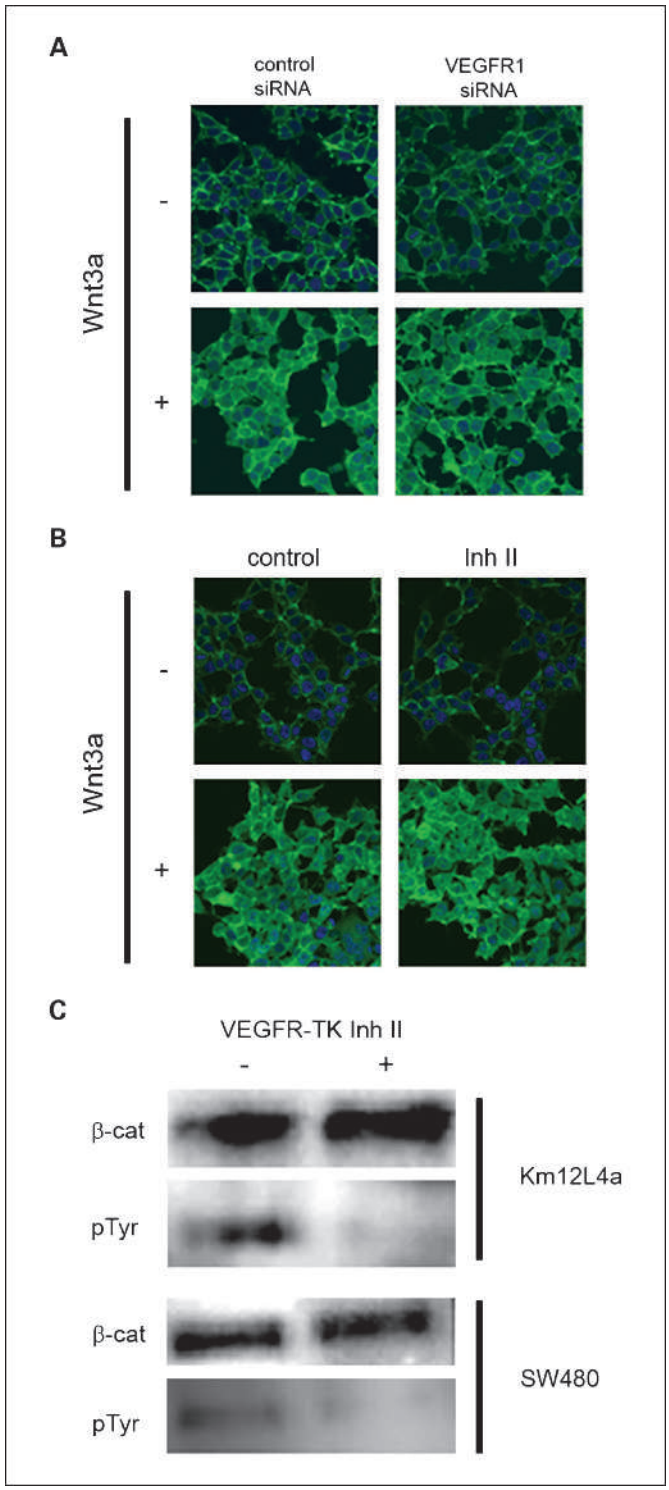

Fig. 6. Modulation of Wnt/β-cat signaling by VEGFR1 is independent of β-cat stabilization and nuclear translocation, but correlates with β-cat tyrosine phosphorylation. *A* and *B,* confocal immunofluorescence microscopy images showing β-cat subcellular localization (*green*) in STF293 cells transfected with either siRNA targeting VEGFR1 or a nontargeting control duplex for 48 h (*A*), or treated with Inh II (1 μmol/L) or vehicle for 18 h (*B*). Cells were stimulated for 2 h with either control media (*top*) or Wnt3a (*bottom*). Nuclei (*blue*) were stained with 4′,6-diamidino-2-phenylindole (magnification, ×40). *C,* western blot analysis of immunoprecipitated β-cat from KM12L4a and SW480 colon carcinoma cells treated with Inh II (1 μmol/L) for 48 h. Samples were first probed with anti–phosphotyrosine (pTyr) antibody, stripped, and reprobed with anti–β-cat antibody.

and nuclear translocation. These data concurred with observations in $Apc^{Min/+}$ mice that showed no change in nuclear β-cat upon treatment with the VEGFR TK inhibitor AZD2171 (27). Together, the above observations suggested that regulation of Wnt/β-cat signaling by VEGFR1 occurred at the level of post-translational modification of β-cat as a transcriptional coregulator and/or subsequent transcriptional activation of a selected subset of β-cat targets.

Preliminary support for VEGFR1-linked effects on post-translational modification of β-cat was provided by analysis of KM12L4a and SW480 colon cancer cells. Inhibition of VEGFR TK activity by treatment with Inh II, followed by immunoprecipitation and western blot analysis of β-cat in both lines, showed a dramatic decrease in tyrosine phosphorylated β-cat. However, β-cat total protein levels, which are canonically governed by phospho-serine/threonine–dependent proteasomal degradation, were found to be unchanged (Fig. 6C). Thus, inhibition of VEGFR1 TK activity resulted in decreased tyrosine phosphorylation of β-cat, thereby abrogating Wnt/β-cat–dependent pro-proliferative transcriptional activity in colon carcinoma cells per se.

Discussion

A systematic yet unbiased screening approach in the context of activated Wnt signaling in human cells has enabled the discovery of novel candidate kinase regulators of the Wnt/β-cat pathway. Whereas the Wnt pathway has been extensively pursued with the use of model organism-based genetic screens, recent observations have found newer positive functions of two classic negative regulators of the Wnt pathway, APC (28) and GSK3β (29), highlighting the inherent epistatic bias of conventional assays (30). By interrogating Wnt signaling at the level of transcriptional activation in human STF293 cells with the use of targeted RNA interference, we hoped to identify novel candidate repressors as well as activators of the Wnt/β-cat pathway, which could be further investigated in cell-specific contexts. Additionally, when establishing a screening strategy, there may be concern that the multitude of altered functional pathways and additional dysregulated kinases in colon cancer cell lines could confound the discovery of Wnt pathway–specific regulators. For a conventional synthetic lethal assay, we reasoned that the likelihood was high that a siRNA library screen would identify candidates that simply killed colon cancer cells through other pathways and hence would give rise to off-target effects instead of direct effects on Wnt-dependent transcription. Thus, starting with STF293 cells, we showed that one identified candidate, VEGFR1/Flt1, was a regulatory target with clinical relevance by examining Wnt/β-cat–dependent transcription in a wide variety of contexts, including genetic-null embryonic cells from a *VEGFR1*$^{-/-}$ mouse, loss-of-function by siRNA and shRNA, VEGFR TK inhibition in Wnt-responsive cells, as well as survival of Wnt/β-cat–addicted colon carcinoma cells.

Our data provide potential mechanistic linkages in support of prior observations. For example, VEGFR1 is expressed in various colon cancer lines that show activated Wnt signaling, including SW480 and KM12L4a cells (21). In addition, preclinical studies of a hexapeptide specifically targeting VEGFR1 (31), as well as the VEGFR TK inhibitors SU11248 (32), AZD2171 (27), and CHIR-258 (33), have shown efficacy in various models of colon cancer; however, whether the mechanism involved therapeutic "anti-angiogenesis" remains unclear (21). Furthermore, we found that VEGFR1-linked regulation of β-cat was found to be independent of GSKβ activity and β-cat nuclear translocation while impacting β-cat tyrosine phosphorylation, thus providing preliminary insight into a mechanism for the antiproliferation action of VEGFR1 inhibition. It is acknowledged that the exact site of tyrosine phosphorylation remains to be mapped, and the potential differential roles of soluble VEGFR1, a splice variant (34), versus full-length VEGFR1 need to be resolved. Nonetheless, the implication that VEGFR1 links TK activity, directly or indirectly, to a node of the Wnt pathway downstream of commonly occurring oncogenic mutations tremendously enhances its potential as a therapeutic target in the context of aberrant Wnt signaling in cancer.

Our siRNA-based high-throughput screen, which uncovered an unanticipated tumor cell linkage between VEGFR1 and Wnt/β-cat, extends the context-dependent cross-talk identified between the oncogenic Flt3 and Wnt pathways in acute myeloid leukemia (35), to VEGFR1/Flt1 and Wnt/β-cat in colon carcinoma. Indeed, comparative genomic hybridization analysis of metastatic human colon cancer shows gain of chromosomes 1p, 8q, 13q, and 20q, including a distinct amplicon ranging from 13q11 to 13q21 (36), a region that overlaps with the exact cytogenetic location of VEGFR1. Thus, our results provide an alternative tumor cell–centric basis for the partial successes of anti-angiogenic therapy being delimited to only a few cancer types, such as colorectal cancer, a Wnt/β-cat–addicted tumor type. Future studies will be pursued to confirm this in clinical specimens in the context of targeted therapy. Potentially, a mechanistically rational strategy for synthetic lethal therapy in the treatment of colon carcinoma is selective targeted suppression of VEGFR1 TK activity in the Wnt/β-cat–addicted tumor cells themselves.

Disclosure of Potential Conflicts of Interest

No potential conflicts of interest were disclosed.

Acknowledgments

We thank Dr. Dustin Maxwell for assistance with immunofluorescence microscopy, Dr. James Hsieh for assistance with reverse transcriptase-PCR profiling, and our colleagues at the Washington University Molecular Imaging Center for discussion.

References

1. Giles RH, van Es JH, Clevers H. Caught up in a Wnt storm: Wnt signaling in cancer. Biochim Biophys Acta 2003;1653:1–24.
2. Clevers H. Wnt/β-catenin signaling in development and disease. Cell 2006;127:469–80.
3. Kaelin WG, Jr. The concept of synthetic lethality in the context of anticancer therapy. Nat Rev Cancer 2005;5:689–98.
4. Willingham AT, Deveraux QL, Hampton GM, Aza-Blanc P. RNAi and HTS: exploring cancer by systematic loss-of-function. Oncogene 2004; 23:8392–400.
5. Hartman JT, Garvik B, Hartwell L. Principles for the buffering of genetic variation. Science 2001; 291:1001–4.
6. Friend S, Oliff A. Emerging uses for genomic information in drug discovery. N Engl J Med 1998; 338:125–6.
7. Gross S, Piwnica-Worms D. Real-time imaging of ligand-induced IKK activation in intact cells and in living mice. Nat Methods 2005;2:607–14.
8. Zhang XD, Yang XC, Chung N, et al. Robust statistical methods for hit selection in RNA interference high-throughput screening experiments. Pharmacogenomics 2006;7:299–309.
9. Xu Q, Wang Y, Dabdoub A, et al. Vascular development in the retina and inner ear: control by

Norrin and Frizzled-4, a high-affinity ligand-receptor pair. Cell 2004;116:883–95.
10. Shibamoto S, Higano K, Takada R, et al. Cytoskeletal reorganization by soluble Wnt-3a protein signalling. Genes Cells 1998;3:659–70.
11. DasGupta R, Kaykas A, Moon RT, Perrimon N. Functional genomic analysis of the Wnt-wingless signaling pathway. Science 2005;308:826–33.
12. Ma Y, Creanga A, Lum L, Beachy PA. Prevalence of off-target effects in Drosophila RNA interference screens. Nature 2006;443:359–63.
13. Firestein R, Bass A, Kim S, et al. CDK8 is a colorectal cancer oncogene that regulates β-catenin activity. Nature 2008;455:547–51.
14. Weinstein IB, Joe AK. Mechanisms of disease: oncogene addiction-a rationale for molecular targeting in cancer therapy. Nat Clin Pract Oncol 2006;3:448–57.
15. de Vries C, Escobedo JA, Ueno H, et al. The fms-like tyrosine kinase, a receptor for vascular endothelial growth factor. Science 1992;255:989–91.
16. Shibuya M. Vascular endothelial growth factor receptor-1 (VEGFR-1/Flt-1): a dual regulator for angiogenesis. Angiogenesis 2006;9:225–30, discussion 31.
17. Jain RK, Duda DG, Clark JW, Loeffler JS. Lessons from phase III clinical trials on anti-VEGF therapy for cancer. Nat Clin Pract Oncol 2006;3:24–40.
18. Fong GH, Rossant J, Gertsenstein M, Breitman ML. Role of the Flt-1 receptor tyrosine kinase in regulating the assembly of vascular endothelium. Nature 1995;376:66–70.
19. Arnold SJ, Stappert J, Bauer A, et al. Brachyury is a target gene of the Wnt/β-catenin signaling pathway. Mech Dev 2000;91:249–58.
20. Bates RC, Goldsmith JD, Bachelder RE, et al. Flt-1-dependent survival characterizes the epithelial-mesenchymal transition of colonic organoids. Curr Biol 2003;13:1721–7.
21. Fan F, Wey JS, McCarty MF, et al. Expression and function of vascular endothelial growth factor receptor-1 on human colorectal cancer cells. Oncogene 2005;24:2647–53.
22. Furet P, Bold G, Hofmann F, et al. Identification of a new chemical class of potent angiogenesis inhibitors based on conformational considerations and database searching. Bioorg Med Chem Lett 2003;13:2967–71.
23. Mikheev AM, Mikheeva SA, Liu B, Cohen P, Zarbl H. A functional genomics approach for the identification of putative tumor suppressor genes: Dickkopf-1 as suppressor of HeLa cell transformation. Carcinogenesis 2004;25:47–59.
24. Verma UN, Surabhi RM, Schmaltieg A, Becerra C, Gaynor RB. Small interfering RNAs directed against β-catenin inhibit the *in vitro* and *in vivo* growth of colon cancer cells. Clin Cancer Res 2003;9:1291–300.
25. Nakamura K, Yamamoto A, Kamishohara M, et al. KRN633: a selective inhibitor of vascular endothelial growth factor receptor-2 tyrosine kinase that suppresses tumor angiogenesis and growth. Mol Cancer Ther 2004;3:1639–49.
26. Cross DA, Culbert AA, Chalmers KA, et al. Selective small-molecule inhibitors of glycogen synthase kinase-3 activity protect primary neurones from death. J Neurochem 2001;77:94–102.
27. Goodlad RA, Ryan AJ, Wedge SR, et al. Inhibiting vascular endothelial growth factor receptor-2 signaling reduces tumor burden in the ApcMin/+ mouse model of early intestinal cancer. Carcinogenesis 2006;27:2133–9.
28. Takacs CM, Baird JR, Hughes EG, et al. Dual positive and negative regulation of wingless signaling by adenomatous polyposis coli. Science 2008;319:333–6.
29. Zeng X, Huang H, Tamai K, et al. Initiation of Wnt signaling: control of Wnt coreceptor Lrp6 phosphorylation/activation via frizzled, dishevelled and axin functions. Development 2008;135:367–75.
30. Huang H, He X. Wnt/β-catenin signaling: new (and old) players and new insights. Curr Opin Cell Biol 2008;2:119–25.
31. Bae DG, Kim TD, Li G, Yoon WH, Chae CB. Anti-flt1 peptide, a vascular endothelial growth factor receptor 1-specific hexapeptide, inhibits tumor growth and metastasis. Clin Cancer Res 2005;11:2651–61.
32. Mendel DB, Laird AD, Xin X, et al. *In vivo* antitumor activity of SU11248, a novel tyrosine kinase inhibitor targeting vascular endothelial growth factor and platelet-derived growth factor receptors: determination of a pharmacokinetic/pharmacodynamic relationship. Clin Cancer Res 2003;9:327–37.
33. Lee SH, Lopes de Menezes D, Vora J, et al. *In vivo* target modulation and biological activity of CHIR-258, a multitargeted growth factor receptor kinase inhibitor, in colon cancer models. Clin Cancer Res 2005;11:3633–41.
34. Huckle WR, Roche RI. Post-transcriptional control of expression of sFlt-1, an endogenous inhibitor of vascular endothelial growth factor. J Cell Biochem 2004;93:120–32.
35. Kajiguchi T, Chung EJ, Lee S, et al. FLT3 regulates β-catenin tyrosine phosphorylation, nuclear localization, and transcriptional activity in acute myeloid leukemia cells. Leukemia 2007;12:2476–84.
36. Platzer P, Upender MB, Wilson K, et al. Silence of chromosomal amplifications in colon cancer. Cancer Res 2002;62:1134–8.